

Original Article

*Shared first authors.

Cite this article: Wang R, Wang C, Zhang G, Mundinano I-C, Zheng G, Xiao Q, Zhong Y (2024). Causal mechanisms of quadruple networks in pediatric bipolar disorder. *Psychological Medicine* **54**, 4713–4724. <https://doi.org/10.1017/S0033291724002885>

Received: 20 April 2024

Revised: 12 August 2024

Accepted: 22 October 2024

First published online: 16 December 2024

Keywords:


dynamic causal modelling (DCM); effective connectivity; parametric empirical Bayes (PEB); pediatric bipolar disorder

Corresponding author:

Yuan Zhong;

Email: zhongyuan@njnu.edu.cn

Causal mechanisms of quadruple networks in pediatric bipolar disorder

Rong Wang^{1,*}, Chun Wang^{2,*}, Gui Zhang¹, Inaki-Carril Mundinano³, Gang Zheng⁴, Qian Xiao⁵ and Yuan Zhong¹ 

¹School of Psychology, Nanjing Normal University, Nanjing 210097, China; ²Department of Psychiatry, Nanjing Brain Hospital Affiliated to Nanjing Medical University, Nanjing 210029, China; ³Cognitive Neuroscience Laboratory, Department of Physiology and Neuroscience Program, Biomedicine Discovery Institute, Monash University, Victoria 3800, Australia; ⁴Monash Biomedical Imaging, Monash University, Victoria 3800, Australia and ⁵Mental Health Centre of Xiangya Hospital, Central South University, Changsha 410008, China

Abstract

Background. Pediatric bipolar disorder (PBD) is characterized by abnormal functional connectivity among distributed brain regions. Increasing evidence suggests a role for the limbic network (LN) and the triple network model in the pathophysiology of bipolar disorder (BD). However, the specific relationship between the LN and the triple network in PBD remains unclear. This study aimed to investigate the aberrant causal connections among these four core networks in PBD.

Method. Resting-state functional MRI scans from 92 PBD patients and 40 healthy controls (HCs) were analyzed. Dynamic Causal Modeling (DCM) was employed to assess effective connectivity (EC) among the four core networks. Parametric empirical Bayes (PEB) analysis was conducted to identify ECs associated with group differences, as well as depression and mania severity. Leave-one-out cross-validation (LOOCV) was used to test predictive accuracy.

Result. Compared to HCs, PBD patients exhibited primarily excitatory bottom-up connections from the LN to the salience network (SN) and bidirectional excitatory connections between the default mode network (DMN) and SN. In PBD, top-down connectivity from the triple network to the LN was excitatory in individuals with higher depression severity but inhibitory in those with higher mania severity. LOOCV identified dysconnectivity circuits involving the caudate and hippocampus as being associated with mania and depression severity, respectively.

Conclusions. Disrupted bottom-up connections from the LN to the triple network distinguish PBD patients from healthy controls, while top-down disruptions from the triple network to LN relate to mood state differences. These findings offer insight into the neural mechanisms of PBD.

Introduction

Bipolar disorder (BD) is a severe neuropsychiatric disorder marked by alternating episodes of mania and depression, with symptom-free periods of euthymia in between (Harrison, Geddes, & Tunbridge, 2018). The latest World Mental Health surveys conducted between 2001 and 2022 reported that the lifetime prevalence of BD is approximately 2% (McGrath et al., 2023; Nierenberg et al., 2023). The probability of first onset of BD peaked at around 15 years, with the median age of onset being approximately 20 years (McGrath et al., 2023). When BD first emerges during childhood or pre-adolescence, it is referred to as pediatric bipolar disorder (PBD) (Harrison et al., 2018).

BD is considered a disconnection syndrome (Perry, Roberts, Mitchell, & Breakspear, 2019; Sha, Wager, Mechelli, & He, 2019), due to disruptions in large-scale networks, as assessed by resting-state functional magnetic resonance imaging (rs-fMRI) (Wu et al., 2023). These disruptions can be further understood by the triple network model, which comprises the default mode (DMN), salience (SN), and central executive (CEN) networks and has been suggested to underlie the pathogenesis of BD (Menon, 2011; Zhang et al., 2022). Abnormal information flow within the CEN and between the CEN and SN is thought to contribute to the working memory deficits frequently observed in BD patients (Dima, Roberts, & Frangou, 2016). In addition, hyperactivity in the DMN has been linked to suppressing task-irrelevant activity during cognitive performance tasks (Zarp Petersen et al., 2022). Indeed, the model proposes that SN is responsible for switching between the DMN and CEN (Goulden et al., 2014). For example, the decreased connectivity between the anterior cingulate cortex (ACC) and insula in SN leads to the abnormal activation of CEN, which compromises cognition and goal-directed behaviors (Menon, 2011). These dysfunctional patterns of connectivity are a recognized cause of cognitive deficits in various neuropsychiatric disorders, such as BD, schizophrenia, depression,

© The Author(s), 2024. Published by Cambridge University Press. This is an Open Access article, distributed under the terms of the Creative Commons Attribution-NonCommercial-ShareAlike licence (<http://creativecommons.org/licenses/by-nc-sa/4.0>), which permits non-commercial re-use, distribution, and reproduction in any medium, provided the same Creative Commons licence is used to distribute the re-used or adapted article and the original article is properly cited. The written permission of Cambridge University Press must be obtained prior to any commercial use.

anxiety, dementia, and autism (Sha *et al.*, 2019). However, this model remains under explained for the state switching in BD.

Recent research has identified the limbic network (LN) as a core site of pathological alterations in BD, suggesting that disruptions in the LN, along with frontal brain regions, play a central role in both cognitive and emotional dysfunctions (Mesbah *et al.*, 2023). Specifically, aberrant interactions between the triple network and LN provide crucial insights into BD symptoms. However, the interaction mechanisms between the LN and the triple network model in PBD remain unclear. Magioncalda and Martino (2022) emphasized that the aberrations in LN trigger abnormal subcortical-cortical coupling, further destabilizing network balance. This process contributes to abnormalities in various dimensions of affectivity, thought, and psychomotor function in different states of BD (Martino & Magioncalda, 2022). Several studies have provided tentative evidence for a top-down pathological alteration from the triple networks toward the LN. Specifically, patients in remission show hyperconnectivity between the ACC/ventromedial PFC (vmPFC) and the LN (Blond, Fredericks, & Blumberg, 2012; Blumberg *et al.*, 2005), while patients in the acute phase show hyperconnectivity between the ACC/dorsomedial prefrontal cortex (dmPFC) and the LN (Gusnard, Akbudak, Shulman, & Raichle, 2001). Most previous studies were based on functional connectivity quantifying statistical dependencies, yet these methods do not explain the causal mechanisms of interaction.

A deeper understanding of the causal interactions between the triple network and LN is essential for clarifying the underlying pathological processes in BD. Considering that childhood and adolescence are the time of increased vulnerability to BD (McGrath *et al.*, 2023) and the development and maturation of brain intrinsic networks (Ahmed, Bittencourt-Hewitt, & Sebastian, 2015), investigating the interaction mechanism of the triple network and LN in PBD is particularly important.

Based on the above, we propose that a quadruple network mechanism, integrating the triple network and the LN, underpins the pathology of PBD. The interaction between these networks could be disentangled into top-down and bottom-up processes using spectral dynamic causal modelling (spDCM) (Sabarodin *et al.*, 2023), shedding light on the debated interactions between the triple network and the LN. Furthermore, parametric empirical Bayes (PEB) can reveal distinct network connections between PBD patients and healthy controls. What's more, PEB can identify different connections between PBD and healthy control (HC) groups (Zeidman *et al.*, 2019a, 2019b), as well as connections associated with symptom severity (Bouziane, Das, Friston, Caballero-Gaudes, & Ray, 2022). We hypothesize that (1) the bottom-up connections from LN to triple networks may represent trait-associated characteristics of PBD, as compared to HC, and (2) top-down connections from triple networks to LN may be associated with symptom-related factors.

Methods and materials

Dataset and participants

Adolescents diagnosed with BD ($N = 92$; age 11–21) (Sawyer, Azzopardi, Wickremarathne, & Patton, 2018; Van Meter, Moreira, & Youngstrom, 2011), were recruited from child and Adolescent Psychiatry Clinics. Age- and sex-matched HC adolescents ($N = 40$) were recruited primarily from public schools through advertisements. Specific exclusion criteria can be found

in the supplementary material. All participants were fully informed of the procedures, and their guardians provided informed consent. This study was approved by the local research ethics board (NJNU-2019-SYLL-018). Licenced child-adolescent psychiatrists conducted semi-structured diagnostic interviews for all participants using the Affective Disorders and Schizophrenia Scale for School-Age Children-Present and Lifetime Version (K-SADS-PL). All diagnoses were confirmed based on DSM-IV criteria.

Demographic and clinical assessments were performed on the same day as neuroimaging. Data was acquired from two sites with different protocols: the Xiangya Second Hospital (XYH) protocol at the Pediatric Psychiatry Clinic of Changsha Xiangya Second Hospital, Hunan province (53PBD, 21HC), and the Nanjing Brain Hospital (NBH) protocol at the Nanjing Brain Hospital Affiliated to Nanjing Medical University in Jiangsu (39PBD, 19HC).

Medication and comorbidity

Across both sites, 49 participants were treated with one or more of the following medications: lithium, valproate, second-generation antipsychotics, and antidepressants. Reported comorbidities included attention deficit hyperactivity disorder (ADHD, $N = 7$), oppositional defiant disorder (ODD, $N = 5$), generalized anxiety disorder (GAD, $N = 3$), and borderline personality disorder (BPD, $N = 1$).

Clinical assessments

The Mood and Feelings Questionnaire (MFQ) and the Young Mania Rating Scale (YMRS) were used to assess depression and manic symptoms in 53 patients at XYH and 3 patients at NBH, respectively. For the remaining 36 patients at NBH, the Hamilton Depression Scale (HAMD) and the Mood Disorder Questionnaire (MDQ) were used to evaluate depressive and manic symptoms, respectively. To maintain the original distribution of scores, Min-Max Normalization (Jain, Nandakumar, & Ross, 2005) was applied to standardize depression and manic scores across a common range. This normalization process was implemented in MATLAB using the code provided by Friedman and Komogortsev (2019).

MRI data acquisition

During the MRI scans, participants were instructed to relax, remain still with closed eyes, and stay awake. Foam padding was used to minimize head movement. MRI data were collected from a 3 T Siemens scanner at the Magnetic Resonance Centers of both NBH and XYH. The parameters for the functional images were as follows: repetition time (TR) = 2000 ms, echo time (TE) = 30 ms, 30 slices, slice thickness = 4.00 mm, gap = 0.4 mm, field of view (FOV) = 240×240 mm, matrix size = 64×64 , and flip angle = 90° . The scan lasted 500 s, capturing 250 volumes at NBH and 240 at XYH.

Preprocessing of rs-fMRI

Preprocessing was performed using DPABI V7.0 (Yan, Wang, Zuo, & Zang, 2016), as follows. The first 10 or 20 images (for NBH and XYH, respectively) of each rs-fMRI session were discarded to ensure steady-state longitudinal magnetization, leaving 230 rs-fMRI volumes for analysis. First, resting-state fMRI images were slice-timing corrected using the central slice of each volume

as the reference. Next, images were realigned to the first functional volume of each session. After realignment, functional and structural T1 images were manually coregistered and transformed from the individual native space to the standard Montreal Neurological Institute (MNI) space. The generated images were spatially smoothed with a Gaussian kernel of 6 mm at full width at half-maximum. The resulting fMRI data were linearly trend removed and band-pass (0.0078–0.1 Hz) filtered to reduce low-frequency drift and high-frequency noise (Almgren et al., 2018). Subsequently, micro-head motion effects were regressed using the Friston-24 head motion parameter model. Mean signals from white matter and cerebrospinal fluid nuisance variables were removed from the preprocessed time courses by multiple linear regression analysis using the SPM12 software package (www.fil.ion.ucl.ac.uk/spm/software/spm12).

For functional connectivity analyses of resting state data, it is crucial to regress out motion and physiological parameters. However, this step is not required for independent component analysis (ICA) since it separates motion and physiological noise as independent components (Goulden et al., 2014).

Independent component analysis

Independent component analysis (ICA) was carried out using the Group ICA of fMRI toolbox (GIFT, <http://mialab.mrn.org/software/gift/>) to identify independent components (ICs) across all 132 participants. Dimension estimation was conducted using the minimum description length criterion (Jafri, Pearlson, Stevens, & Calhoun, 2008), to determine the optimal number of ICs for the datasets from the three groups. A template-matching procedure was then employed to select the components with the highest spatial correlation to the DMN, CEN, SN, and LN.

The GIFT toolbox provides Resting State Network (RSN) templates derived from resting-state data. DMN, SN, and CEN templates were obtained from the Functional Imaging Unit at the Neuropsychiatric Disorders Laboratory at Stanford University, California (http://findlab.stanford.edu/functional_ROIs). In line with previous studies (Bryant et al., 2005; Tost et al., 2010), the LN template was constructed using the Wake Forest University (WFU) PickAtlas utility (<http://www.fmri.wfubmc.edu/>). This LN template included key regions such as the temporal pole, orbitofrontal cortex (OFC) (Schaefer et al., 2018); hippocampus, amygdala, parahippocampus, and striatum (Catani, Dell'Acqua, & Thiebaut De Schotten, 2013).

To visualize the spatial distribution of each network's independent components across participants, one-sample *t* tests were conducted using SPM12 (<http://www.fil.ion.ucl.ac.uk/spm/>).

Dynamic causal modeling

DCM estimates the causal architecture (effective connectivity) of distributed neuronal responses from observed BOLD (Blood-Oxygen-Level-Dependent) signals recorded from fMRI.

For the preprocessed rs-fMRI data, fully connected intrinsic DCMs were specified in SPM12 (v7771) (http://www.fil.ion.ucl.ac.uk/spm/spm_dcm_specify.m) using 18 regions of interest (ROIs), with 6 mm radius spheres centered on the ICA-derived MNI coordinates. ComBat harmonization (Fortin et al., 2017, 2018; Johnson, Li, & Rabinovic, 2007) was applied to correct for scanner site effects on the DCM indices after model specification.

After extracting the rs-fMRI time series from the ROIs, we used cross-spectral DCM (Zeidman et al., 2019a; *spm_dcm_fit.m*)

to estimate each subject's pairwise effective connectivity. The theoretical foundation and optimization process of DCM are provided in the supplementary materials. We performed a diagnostic test for each DCM (*spm_dcm_fmri_check.m*) to evaluate both model convergence and accuracy of the model inversion by assessing the percentage of variance explained by the DCM model when fitted to the observed cross-spectral data. All models showed reliable results, with no participant having less than 10% variance explained (Zeidman et al., 2019a).

PEB for group DCM

After inverting each subject's fully connected DCM, a Parametric Empirical Bayes (PEB) analysis was conducted to estimate group-level effective connectivity (EC), group differences, and the linear relationship between symptom severity reports and each EC link (Zeidman et al., 2019b; *spm_dcm_peb.m*). This was done using a general linear model (GLM) based on subject-specific parameters. The expected values and the associated uncertainty (posterior covariance) of the parameters for each connection were then analyzed at the between-subject or group level (Zeidman et al., 2019b). Further details of these analyses are provided in the supplementary materials.

To assess effective connectivity strength from a network perspective, Bayesian contrasts were used to compute the averaged network ECs, taking into account the full posterior distribution of each EC parameter rather than relying on the arithmetic mean of parameter expectations (Nicenboim, Schad, & Vasisht, 2023, <https://github.com/bnicenboim/bcogsci>). This approach was also applied in previous studies (Zhang et al., 2022; Zhou et al., 2018). Please see the supplementary for specific procedure.

Leave-one-out cross validation analysis

We tested whether depression and mania scores, as well as group differences, could be predicted from subject-specific estimates of effective connectivity (EC) using a leave-one-out cross-validation (LOOCV) analysis (Friston et al., 2016; Zeidman et al., 2019b), implemented in SPM12 (*spm_dcm_loo.m*). To focus on the EC parameters with the strongest evidence of being non-zero, we applied a threshold of 95% posterior probability for inclusion, following previous approaches. The parameters were estimated using Bayesian Model Averaging (BMA); further details can be found in the supplementary materials. In each iteration, one participant was left out, and a PEB model was inverted to predict the left-out subject's score based on the selected EC connections (Bouziiane et al., 2022).

NeuroSynth

Cognitive terms associated with the brain regions most predictive in the LOOCV analysis were identified using the NeuroSynth database based on a set of 400 topic terms (<https://github.com/neurosynth/neurosynth>). An automated parsing method, relying on multiple association metrics, was applied to extract psychological and cognitive terms from this pool. The results were organized using a posterior probability matrix (Lu et al., 2022).

Results

Demographic variables

Table 1 summarizes the demographic and clinical characteristics of the participants. There were no significant differences in age or gender distribution between the PBD and HC groups.

Table 1. Demographic and clinical characteristics of participants

Characteristics	PBD (N = 92)	HC (N = 40)	t/χ^2	p
Age (years)	16.21 ± 2.40*	16.05 ± 2.94*	0.32 ^a	0.75
Gender (F/M)	62/30	29/11	0.34 ^b	0.56
Comorbidity (T/F)	16/76	NA	NA	NA
Medicine (T/F)	49/43	NA	NA	NA
raw HAMD/MFQ	32.14 ± 10.10* (N = 36)/14.66 ± 13.99* (N = 56)	NA		NA
normalization HAMD/MFQ	0.52 ± 0.23* (N = 36)/0.28 ± 0.29* (N = 56)	NA	NA	NA
raw MDQ/YMRS	5.54 ± 3.00* (N = 36)/14.45 ± 13.53* (N = 56)	NA	NA	NA
Normalization MDQ/YMRS	0.43 ± 0.23* (N = 36)/0.31 ± 0.31*(N = 56)	NA	NA	NA

Abbreviation: PBD, Pediatric Bipolar Disorder; HC, healthy control; HAMD, Hamilton depression scale; MDQ, Mood Disorder Questionnaire; MFQ, Mood and Feelings Questionnaire; YMRS, Young Mania Rating Scale.
*Mean ± s.d.
^aThe p value was obtained by a two-sample t test.
^bThe p value was obtained by a χ^2 test.

Resting state network spatial distribution map

ICA revealed 25 independent components, five of which were identified as corresponding to the DMN ($r = 0.47$), left and right CEN ($r = 0.37$ for both), SN ($r = 0.42$), and LN ($r = 0.19$), based on template matching analysis. The spatial distribution of these five RSNs was illustrated by the results of a one-sample t test (Fig. 1). The DMN ROIs consisted of subgenual ACC (sgACC, anterior DMN), angular and combined posterior cingulate cortex-precuneus (PCC-Precun) (posterior DMN), according to Clancy *et al.* (2023); Yokoyama *et al.* (2018); Zhang and Raichle (2010). The ROIs of the CEN were located in dorsolateral frontal (including middle frontal gyrus, MFG) and parietal (including parietal lobule, IPL) neocortices (Feng *et al.*, 2021; Liu *et al.*, 2021; Seeley *et al.*, 2007). The SN was anchored by the dorsal ACC (dACC) and the anterior insula (AI) (Hogeveen, Krug, Elliott, & Solomon, 2018; Seeley *et al.*, 2007). The LN included the hippocampus, amygdala, and caudate (Lim *et al.*, 2013; Ong *et al.*, 2012). The key brain regions included in each network are listed in Table 2.

Similarity and group comparison of the causal connections across HCs and PBDs

The group-mean effective connectivity results are shown in panels A and B(a) of Fig. 2 (free energy threshold, Bayesian posterior probability > 0.95). In the triple network model, the connections between the CEN and DMN and from the CEN to the SN were generally inhibitory. Specifically, inhibitory connections were observed from the right MFG to the sgACC and dACC, from the left IPL to the right angular gyrus, and from the PCC-Precun to the IPL. In contrast, connections between the DMN and LN, the CEN and LN, and the SN and LN shared similar excitatory patterns, suggesting that the triple networks may interact collectively with the LN.

Panels A and B(b) of Fig. 2 (free energy threshold, 95%) show group-specific differences in effective connectivity. In the PBD group, dysfunctional connections were observed from the LN to the SN, within the SN, and between the DMN and SN.

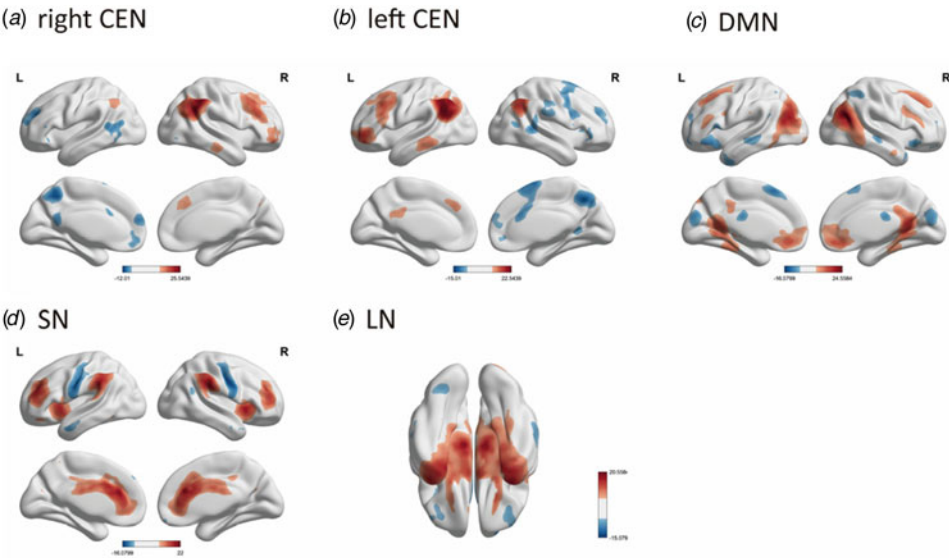


Figure 1. Results of one-sample t test in 5 RSNs of all subjects, shown by BrainNet Viewer. (a), (b), (c), (d), AND (e) respectively demonstrates the DMN, left/right CEN, SN, LN ($p < 0.05$, FEW corrected).

Table 2. The peak MNI coordinates of the 18 group-level regions of interest

Network	num	Brain region	MNI coordinates (x,y,z)	t value	<i>p</i> FWE-corr
DMN	1	sgACC	3, 36, -9	13.33	< 0.001
	2	PCC-Precun	-3, -54, 9	19.94	< 0.001
	3	Angular_R	45, -66, 30	17.94	< 0.001
	4	Angular_L	-42, -66, 33	11.75	< 0.001
CEN	5	MFG_R	39, 27, 30	18.53	< 0.001
	6	MFG_L	-39, 30, 33	12.51	< 0.001
	7	IPL_R	51, -45, 45	25.15	< 0.001
	8	IPL_L	-45, -51, 42	19.84	< 0.001
SN	9	dACC_R	6, 27, 21	21.05	< 0.001
	10	dACC_L	-6, 30, 21	20.45	< 0.001
	11	AI_R	39, 12, 0	17.04	< 0.001
	12	AL_L	-36, 12, 0	17.66	< 0.001
LN	13	Caudate_R	12, 9, 3	21.79	< 0.001
	14	Caudate_L	-12, 12, 0	18.85	< 0.001
	15	Hippocampus_R	33, -18, -6	11.03	< 0.001
	16	Hippocampus_L	-21, -21, -12	9.95	< 0.001
	17	Amygdala_R	27, 6, -15	12.22	< 0.001
	18	Amygdala_L	-24, 0, -12	13.94	< 0.001

Changes in effective connectivity with depression and mania scores

Panel C of Fig. 2 shows the specific connections significantly associated with depression and mania scores. To visualize the changes at the network level, average values within each submatrix were calculated using Bayesian contrasts (see panel D of Fig. 2).

In subjects with higher depression severity, connections within the CEN, DMN, and LN were more excitatory, while inter-network connections among the triple networks were more inhibitory. Additionally, connections from the triple networks to the LN were more excitatory. In contrast, patients with higher mania scores exhibited an almost opposite polarity (see panel D(c) of Fig. 2).

Both manic and depressive symptoms showed a similar pattern in terms of LN-to-triple network connections. Specifically, the LN exerted inhibitory effects on the DMN and SN but excitatory effects on the CEN, as shown in panel D(d) of Fig. 2.

Cross validation

In the LOOCV of all connections significantly associated with depression or mania scores or showing significant group differences, several connections were found to predict depression and mania scores, as well as group differences, at a significance level of $\alpha = 0.05$ (see online Supplementary SI Table S2, Fig. 3). The dysconnectivity circuits in PBD, compared to HCs, were predominantly related to the LN, which accounted for 3/4 of the significant connections.

The LOOCV analysis for predicting mania severity revealed that 5 out of 6 connections were associated with the caudate, involving mutually inhibitory relationships between the caudate and angular gyrus, as well as between the caudate and hippocampus. Similarly, the LOOCV analysis for predicting depression

severity indicated that the hippocampus was the only region with abnormal connectivity across all three networks (see online Supplementary Fig. S1).

Meta-analysis cognitive terms relevant to caudate and hippocampus

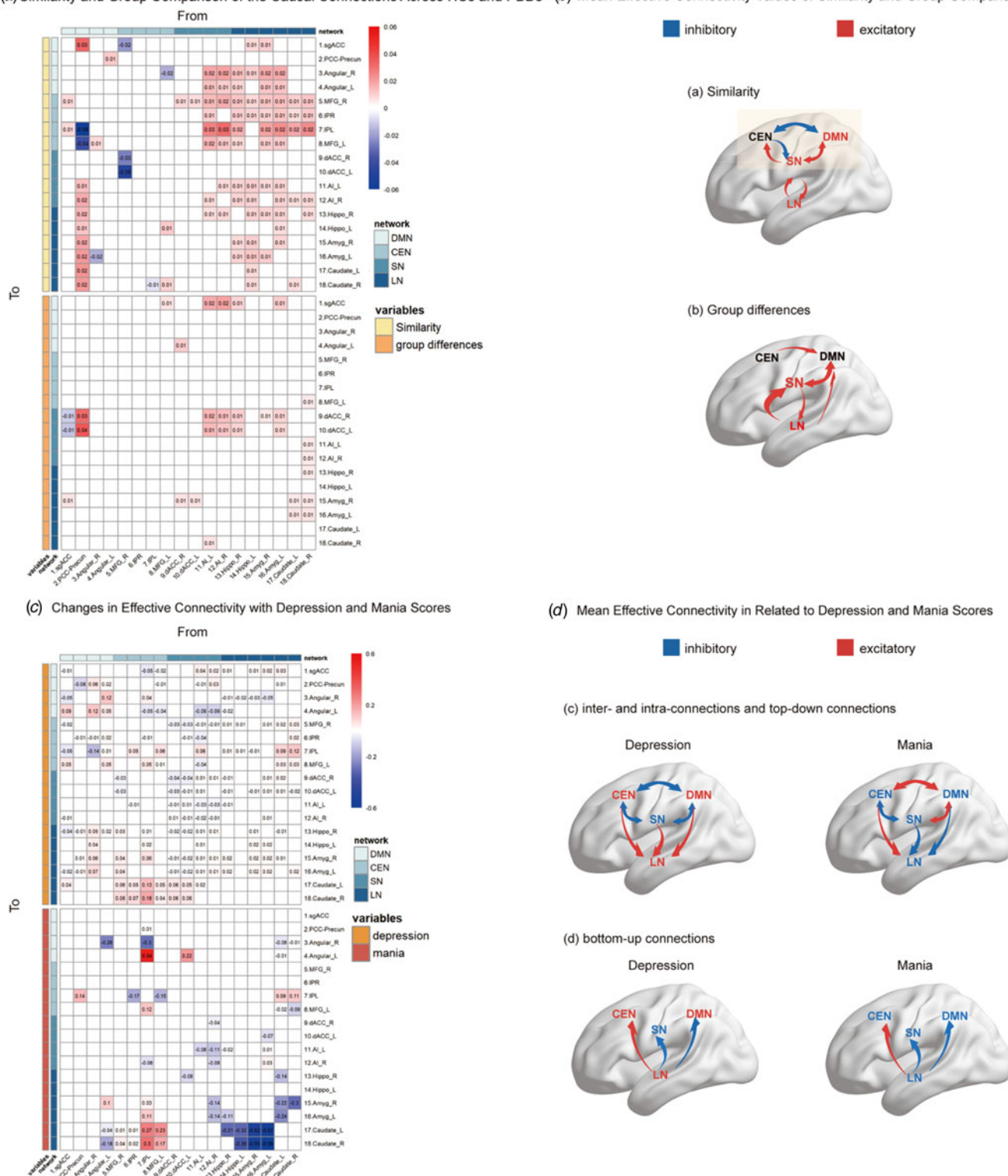
Cognitive associations related to the caudate and hippocampus were identified through automatic parsing in NeuroSynth. The different top terms generated may suggest distinct aspects of symptoms in PBD, as reflected by the two sets of coordinates (Fig. 4 and online Supplementary SI Fig. S2), corresponding to mania and depression, respectively.

Discussion

PBD is widely recognized as a dysconnectivity disorder, as supported by numerous (Luciano et al., 2023). However, a detailed characterization of the causal influences in PBD and their correlations with symptoms has been lacking. This study demonstrated that the core pathological alteration in PBD lies in the disruption of bottom-up connections from the LN to the SN, as well as in the connections between the SN and DMN, compared to HC. Additionally, significant correlations between brain activity and mood states – specifically depression and mania – were primarily observed in the hippocampus and caudate regions. The differences between brain activity related to depression and mania were predominantly found in the top-down connectivity from the triple network to the LN. Furthermore, we replicated the previously reported bidirectional abnormal interactions within the triple network model (Lopez-Larson et al., 2017; Zhang et al., 2022).

We observed that the four core networks shared similar interaction patterns across HCs and PBD patients. The connection

(a) Similarity and Group Comparison of the Causal Connections Across HCs and PBDs (b) Mean Effective Connectivity Values of Similarity and Group Comparison

**Figure 2.** Effective connectivity.

Panel A shows the group-common and group-differences effects of EC (Hz) where the posterior probability exceeds 95% (strong evidence). Panel B shows the mean effective connectivity values from Panel A, viewed from a network perspective and calculated using Bayesian contrast, with an estimated error of less than 0.05. Panel C shows the relationship between symptom severity and EC in the PBD group ($N = 92$), where the posterior probability is greater than 95% (strong evidence). Panel D represents symptom severity associated with the averaged EC in PBD, computed through Bayesian contrast, with an estimated error of less than 0.05.

between the DMN and CEN exhibited a mutual inhibitory influence, which is in line with previous findings in healthy volunteers (Sharaev, Zavyalova, Ushakov, Kartashov, & Velichkovsky, 2016;

Uddin, Clare Kelly, Biswal, Xavier Castellanos, & Milham, 2009; Zhou et al., 2018) and BD patients (Zhang et al., 2022). It is widely accepted that the DMN is a distributed network of brain

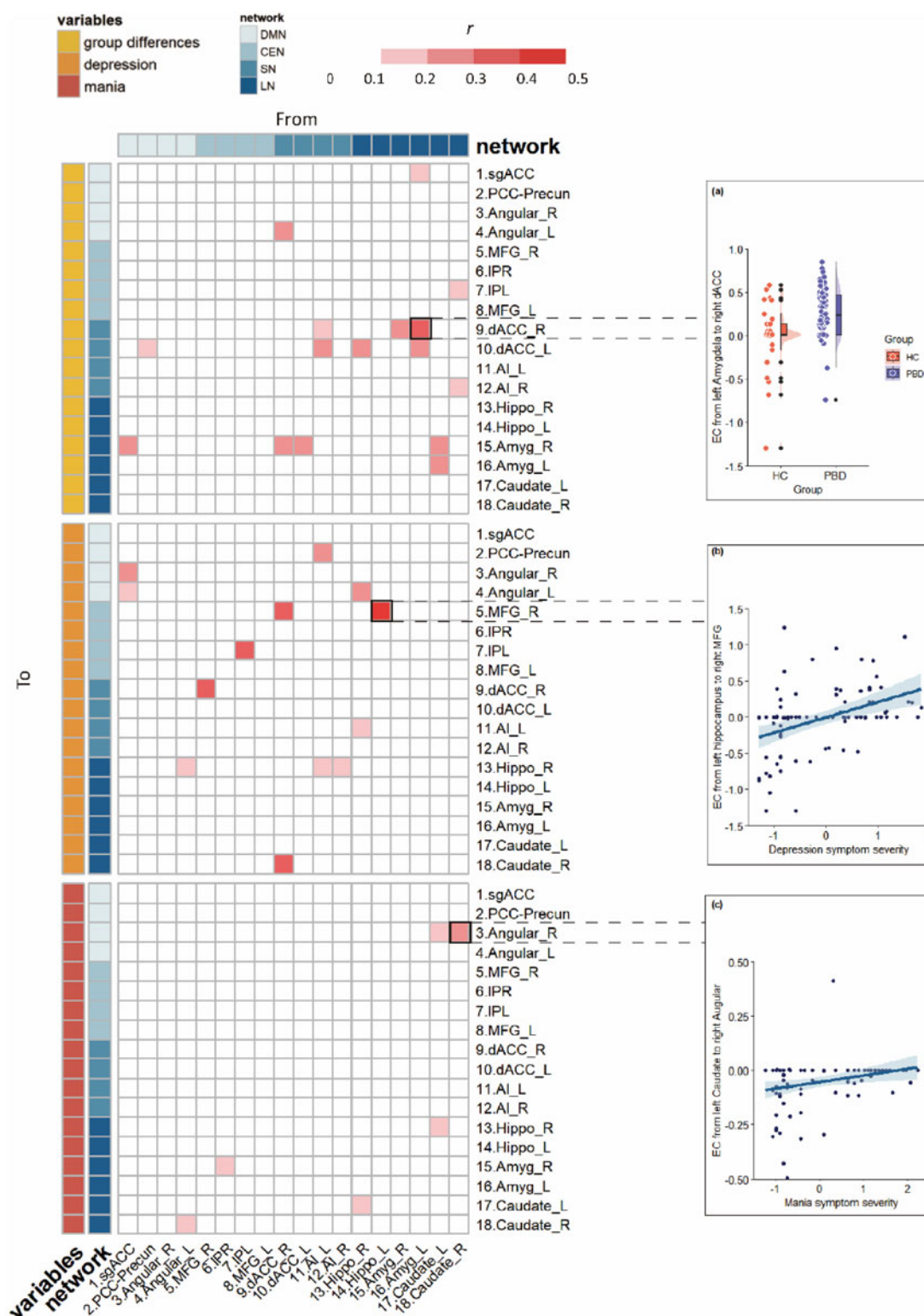


Figure 3. The results of LOOCV.

Left panel: Several connections were found to predict depression and mania scores, and group differences at a significant level of $\alpha = 0.05$.

Right panel: Distributions of certain ECs with significant prediction ability. (a) Shows the excitatory EC from the left Amygdala to the right dACC in HC and PBD groups. (b) Relationship between excitatory EC from left hippocampus to MFG and depression scores. The scatter points and regression line (90% confidence interval, shaded area) depict the association. (c) Relationship between inhibitory EC from right caudate to right angular and mania scores, illustrated by scatter points, regression line, and 90% confidence interval.

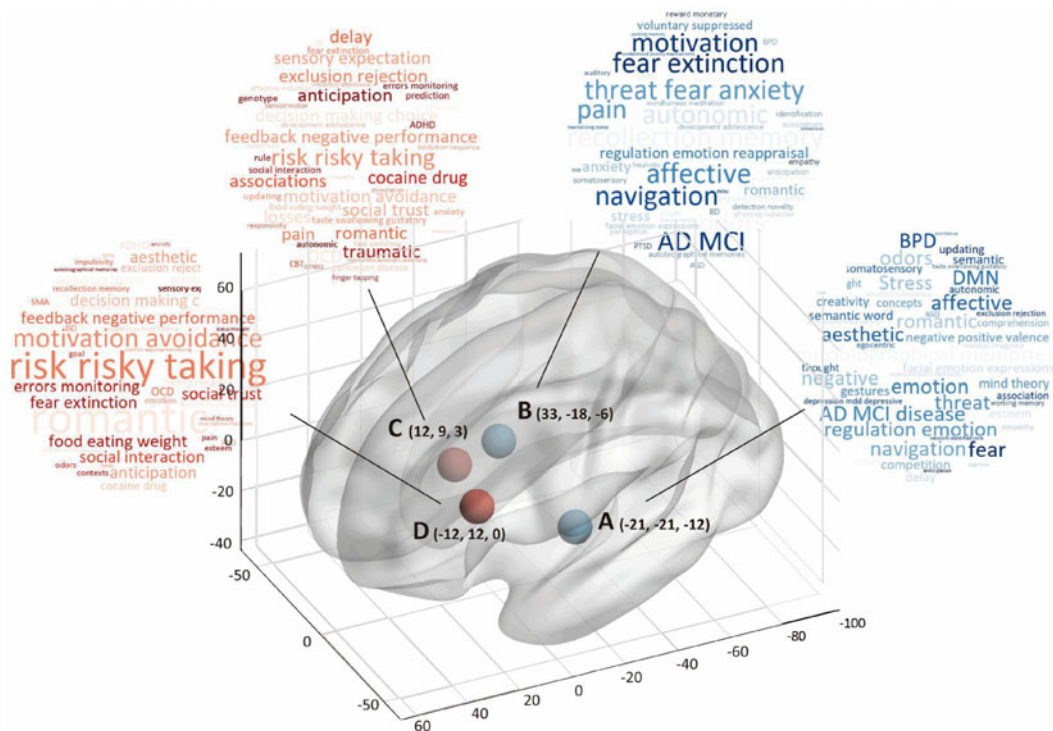


Figure 4. Cognitive terms of hippocampus (A, B) and caudate (C, D). Specific coordinates were selected by independent component analysis in Table 2.

regions more active during rest than during the performance of many attention-demanding tasks (Menon, 2023; Mittner, Hawkins, Boekel, & Forstmann, 2016; Whitfield-Gabrieli & Ford, 2012). Conversely, as part of a complex high-level cognitive network, the CEN shows increased activation during stimulus-driven cognitive or affective processing (Cole & Schneider, 2007; Dosenbach et al., 2007; Sridharan, Levitin, & Menon, 2008). Thus, an anticorrelation relationship between the DMN and CEN is commonly observed (Fox et al., 2005; Greicius, Krasnow, Reiss, & Menon, 2003; Kucyi & Davis, 2014; Molnar-Szakacs & Uddin, 2022).

Importantly, the bidirectional connections between the DMN and LN, CEN and LN, and SN and LN were similarly excitatory. This consistent pattern suggests that the LN may interact with the triple network model as a unified system. One potential explanation for this interaction is the functional differences between these regions. Previous studies have shown that activations in LN with subcortical regions are primarily involved in generating and modulating emotions, while cortical regions play a crucial role in regulating and controlling emotional responses (Bi, Che, & Bai, 2022; Dickstein et al., 2010).

Intrinsic large-scale networks are crucial for understanding the brain alterations in PBD, making group differences particularly important. Compared to HCs, several connections between cortical (DMN, CEN, SN) and subcortical (LN) regions were identified as dysfunctional in PBD patients, primarily in bottom-up connections from the LN to the SN. Notably, these included excitatory connections from the hippocampus and amygdala to the dACC and from the caudate to the AI. The LN has been identified as a core site of pathological alteration in BD, driving abnormal subcortical-cortical coupling and changes in network activity (Magioncalda & Martino, 2022). Furthermore, the SN is built around limbic structures, particularly the dACC and insula (Craig, 2002; Critchley, 2005; Damasio, 2000; Mesulam, 1998),

which integrate highly processed sensory data with visceral, autonomic, and hedonic markers (Damasio, 2000; Seeley et al., 2007). These brain regions significantly contribute to psychiatric disorders by linking subcortical and cortical areas (Rocchi et al., 2020). Therefore, we propose that this abnormal process reflects the LN driving network activity changes through the SN, consistent with the three-dimensional model for BD suggested by Martino and Magioncalda (2022) and the triple network model proposed by Menon (2011).

Consistent with prior research, PBD patients primarily exhibited abnormal effective connectivity (EC) between the DMN and SN compared to HCs, particularly in the inhibitory connection from the sgACC to the dACC, and excitatory connections from the PCC to the dACC, the right dACC to the right angular gyrus, and from the AI to the sgACC. These findings are broadly in line with previous studies reporting atypical increases in functional connectivity between the DMN and SN in both resting-state and task-based fMRI, involving regions such as the dACC, PCC, AI, and mPFC (sgACC) (Dickstein et al., 2007; Gogtay et al., 2007; Lyoo et al., 2006; Murray, Wise, & Graham, 2017; Najt et al., 2007; Pavuluri, O'Connor, Haral, & Sweeney, 2007; Wilke, Kowatch, DelBello, Mills, & Holland, 2004). We speculate that the disrupted development of spatially segregated networks, such as the SN and DMN, in PBD patients may reflect delayed brain maturation compared to healthy children and adolescents (Fair et al., 2009; Lopez-Larson et al., 2017; Power, Fair, Schlaggar, & Petersen, 2010). For instance, alterations in the connections between the ACC and PCC could lead to excessive focus on external stimuli, potentially contributing to manic phases (Magioncalda et al., 2015; Rey et al., 2016; Zovetti et al., 2020).

Cross-validation using a PEB framework tested whether group differences could be predicted based on the effective connectivity estimates of individual subjects (Bouziane et al., 2022; Friston

et al., 2016). Notably, 16 individual connections from the four core networks significantly predicted group differences, indicating that EC accounted for a substantial portion of the between-group variance. Crucially, 12 out of the 16 connections involved regions within the LN, further emphasizing the central role of the LN in PBD.

PBD patients with higher levels of depression exhibited more excitatory causal connections from the triple networks to the LN. In contrast, those with higher levels of mania showed more inhibitory causal connections from the triple networks to the LN. These reversed polarity connections were primarily observed in connections from DMN and SN with LN.

Previous studies have reported changes in resting-state functional connectivity (rsFC) between the DMN and LN (Liu et al., 2013; Liu, Pu, Wu, Zhao, & Xue, 2019; Phillips, Drevets, Rauch, & Lane, 2003; Wu et al., 2023), and between the SN and LN (Chang, Wang, Wu, Lin, & Wang, 2023; Magioncalda & Martino, 2022; Martino & Magioncalda, 2022), in manic and depressive states. However, these studies primarily focused on undirected functional connectivity and rarely examined the interactions from a network perspective. The findings of this study suggest that state-related differences in brain regions occurred predominantly in the top-down connections from the triple networks to LN.

The LOOCV analysis for predicting mania severity revealed that 5 out of 6 significant connections were related to the caudate (see online Supplementary Fig. S1). To our knowledge, few studies have examined causal connectivity associated with mania in BD. The strong link between mania severity and caudate-related causal connectivity identified here may align with evidence suggesting a central role for the caudate in the pathogenesis of mania (Starkstein et al., 1990, 1991). A consistent finding derived from traditional symptom localization in brain lesion studies – which also provides causal inferences (Fox, 2018), revealed a close relationship between caudate lesions and mania symptoms. One possible explanation is that, in the neurobiology of BD, the striatum integrates cognitive and affective processes within cortico-striatal-limbic loops, including the circuits that support emotion regulation (Lei et al., 2023; McKenna & Eyler, 2012). The caudate is a key node within this striatal circuitry, neurobiologically involved in disturbed emotional reactivity, impaired emotion regulation, and impulse control (Phillips & Swartz, 2014; Swann, Lijffijt, Lane, Steinberg, & Moeller, 2009; Wessa, Perlini, & Brambilla, 2015).

The LOOCV analysis for predicting depression severity revealed that the hippocampus was the only region exhibiting abnormal connectivity with all three networks (see online Supplementary Fig. S1). Treatments targeting the hippocampus, such as ketamine and electroconvulsive therapy, have been shown to be effective in treating depression in BD (Wade et al., 2022). Causal structural covariance network analysis, using Granger causality on sequenced T1-weighted images, demonstrated that depression-related alterations often originate from the hippocampus and causally influence the dlPFC and DMN (Han et al., 2023; Li et al., 2019). Additionally, the insula is crucial in mediating the modulation of the precuneus by the hippocampus. Intervention studies, such as transcranial magnetic stimulation (TMS), further support the causal link between activity in these connections and depression symptoms (Philip et al., 2018).

The meta-analysis results also confirmed the relevance of the caudate and hippocampus to mania and depression severity, respectively (Fig. 4). For instance, cognitive terms associated

with the caudate included risk-taking, goal-directed activity, BD, and emotion. In contrast, terms linked to the hippocampus included affective processes, BD, depression, emotion, DMN, and emotional regulation.

There are some limitations in our study. First, while this research provides new insights into alterations in causal connections among the four core networks in PBD patients, the key nodes of each network were selected based solely on previous studies of PBD due to computational constraints. Additionally, since several PBD patients were on medication, and although regression was performed to account for this as a nuisance covariate, further investigation into the specific effects of treatment on EC is warranted.

Conclusion

In summary, the relationship between the triple network and the LN may reflect an essential marker of PBD. The group differences observed are linked to an abnormal process, primarily driven by the LN, which triggers changes in network activity, particularly through its bottom-up influence on the SN. More importantly, the differences in brain activity between depressive and manic mood states are predominantly found in the top-down connectivity from the triple network to the LN. Additionally, the aberrant effective connectivity, particularly involving the hippocampus and caudate, may have pathophysiological relevance for the severity of depression and mania.

Supplementary material. The supplementary material for this article can be found at <https://doi.org/10.1017/S0033291724002885>

Acknowledgements. The authors thank Dr Yuan Zhou (Beijing Anding Hospital) for the code script of Bayesian Contrast analysis. Further, the authors thank Dr Takuya Ishida and Dr Shinsuke Koike (University of Tokyo) for the script of SPM batching analysis of ROIs. ZHENG, G would like to thank the support of the Australian National Imaging Facility Fellowship.

Author contributions. WR methodology, visualization, writing-original draft, writing-review & editing. WC data curation, writing-review & editing. ZHANG, G methodology, writing-review & editing. ICM writing-review & editing. ZHENG, G writing-review & editing. XQ data curation, funding acquisition. ZY conceptualization, methodology, project administration, data curation, funding acquisition, supervision, project administration.

Funding statement. This research was funded by the National Key R&D Program of China (Grant No. 2023YFC3341300), Natural Science Foundation of Jiangsu Province (No. BK20241881), the National Natural Science Foundation of China (No. 81871344, 82201702) and “333 Talent Project” of Jiangsu Province.

Competing interests. None.

Code availability. All code used in this study is available at [GitHub](https://github.com).

References

- Ahmed, S. P., Bittencourt-Hewitt, A., & Sebastian, C. L. (2015). Neurocognitive bases of emotion regulation development in adolescence. *Developmental Cognitive Neuroscience*, 15, 11–25. <https://doi.org/10.1016/j.dcn.2015.07.006>
- Almgren, H., Van De Steen, F., Kühn, S., Razi, A., Friston, K., & Marinazzo, D. (2018). Variability and reliability of effective connectivity within the core default mode network: A multi-site longitudinal spectral DCM study. *NeuroImage*, 183, 757–768. <https://doi.org/10.1016/j.neuroimage.2018.08.053>
- Bi, B., Che, D., & Bai, Y. (2022). Neural network of bipolar disorder: Toward integration of neuroimaging and neurocircuit-based treatment strategies.

- Translational Psychiatry*, 12(1), 143. <https://doi.org/10.1038/s41398-022-01917-x>
- Blond, B. N., Fredericks, C. A., & Blumberg, H. P. (2012). Functional neuroanatomy of bipolar disorder: Structure, function, and connectivity in an amygdala–anterior paralimbic neural system. *Bipolar Disorders*, 14(4), 340–355. <https://doi.org/10.1111/j.1399-5618.2012.01015.x>
- Blumberg, H. P., Donegan, N. H., Sanislow, C. A., Collins, S., Lacadie, C., Skudlarski, P., ... Krystal, J. H. (2005). Preliminary evidence for medication effects on functional abnormalities in the amygdala and anterior cingulate in bipolar disorder. *Psychopharmacology*, 183(3), 308–313. <https://doi.org/10.1007/s00213-005-0156-7>
- Bouziene, I., Das, M., Friston, K. J., Caballero-Gaudes, C., & Ray, D. (2022). Enhanced top-down sensorimotor processing in somatic anxiety. *Translational Psychiatry*, 12(1), 295. <https://doi.org/10.1038/s41398-022-02061-2>
- Bryant, R. A., Felmingham, K. L., Kemp, A. H., Barton, M., Peduto, A. S., Rennie, C., ... Williams, L. M. (2005). Neural networks of information processing in posttraumatic stress disorder: A functional magnetic resonance imaging study. *Biological Psychiatry*, 58(2), 111–118. <https://doi.org/10.1016/j.biopsych.2005.03.021>
- Catani, M., Dell'Acqua, F., & Thiebaut De Schotten, M. (2013). A revised limbic system model for memory, emotion and behaviour. *Neuroscience & Biobehavioral Reviews*, 37(8), 1724–1737. <https://doi.org/10.1016/j.neubiorev.2013.07.001>
- Chang, Z., Wang, X., Wu, Y., Lin, P., & Wang, R. (2023). Segregation, integration and balance in resting – state brain functional networks associated with bipolar disorder symptoms. *Human Brain Mapping*, 44(2), 599–611. <https://doi.org/10.1002/hbm.26087>
- Clancy, K. J., Devignes, Q., Kumar, P., May, V., Hammack, S. E., Akman, E., ... Rosso, I. M. (2023). Circulating PACAP levels are associated with increased amygdala-default mode network resting-state connectivity in posttraumatic stress disorder. *Neuropsychopharmacology*, 48(8), 1245–1254. <https://doi.org/10.1038/s41386-023-01593-5>
- Cole, M. W., & Schneider, W. (2007). The cognitive control network: Integrated cortical regions with dissociable functions. *NeuroImage*, 37(1), 343–360. <https://doi.org/10.1016/j.neuroimage.2007.03.071>
- Craig, A. D. (2002). How do you feel? Interception: The sense of the physiological condition of the body. *Nature Reviews Neuroscience*, 3(8), 655–666. <https://doi.org/10.1038/nrn894>
- Critchley, H. D. (2005). Neural mechanisms of autonomic, affective, and cognitive integration. *Journal of Comparative Neurology*, 493(1), 154–166. <https://doi.org/10.1002/cne.20749>
- Damasio, A. R. (2000). *The feeling of what happens: Body and emotion in the making of consciousness* (1. Harvest ed). New York: Harcourt.
- Dickstein, D. P., Finger, E. C., Skup, M., Pine, D. S., Blair, J. R., & Leibenluft, E. (2010). Altered neural function in pediatric bipolar disorder during reversal learning. *Bipolar Disorders*, 12(7), 707–719. <https://doi.org/10.1111/j.1399-5618.2010.00863.x>
- Dickstein, D. P., Rich, B. A., Roberson-Nay, R., Berghorst, L., Vinton, D., Pine, D. S., & Leibenluft, E. (2007). Neural activation during encoding of emotional faces in pediatric bipolar disorder. *Bipolar Disorders*, 9(7), 679–692. <https://doi.org/10.1111/j.1399-5618.2007.00418.x>
- Dima, D., Roberts, R. E., & Frangou, S. (2016). Connectomic markers of disease expression, genetic risk and resilience in bipolar disorder. *Translational Psychiatry*, 6(1), e706–e706. <https://doi.org/10.1038/tp.2015.193>
- Dosenbach, N. U. F., Fair, D. A., Miezin, F. M., Cohen, A. L., Wenger, K. K., Dosenbach, R. A. T., ... Petersen, S. E. (2007). Distinct brain networks for adaptive and stable task control in humans. *Proceedings of the National Academy of Sciences*, 104(26), 11073–11078. <https://doi.org/10.1073/pnas.0704320104>
- Fair, D. A., Cohen, A. L., Power, J. D., Dosenbach, N. U. F., Church, J. A., Miezin, F. M., ... Petersen, S. E. (2009). Functional brain networks develop from a “local to distributed” organization. *PLoS Computational Biology*, 5(5), e1000381. <https://doi.org/10.1371/journal.pcbi.1000381>
- Feng, C., Eickhoff, S. B., Li, T., Wang, L., Becker, B., Camilleri, J. A., ... Luo, Y. (2021). Common brain networks underlying human social interactions: Evidence from large-scale neuroimaging meta-analysis. *Neuroscience and Biobehavioral Reviews*, 126, 289–303.
- Fortin, J.-P., Cullen, N., Sheline, Y. I., Taylor, W. D., Aselcioglu, I., Cook, P. A., ... Shinohara, R. T. (2018). Harmonization of cortical thickness measurements across scanners and sites. *NeuroImage*, 167, 104–120. <https://doi.org/10.1016/j.neuroimage.2017.11.024>
- Fortin, J.-P., Parker, D., Tunç, B., Watanabe, T., Elliott, M. A., Ruparel, K., ... Shinohara, R. T. (2017). Harmonization of multi-site diffusion tensor imaging data. *NeuroImage*, 161, 149–170. <https://doi.org/10.1016/j.neuroimage.2017.08.047>
- Fox, M. D. (2018). Mapping symptoms to brain networks with the human connectome. *New England Journal of Medicine*, 379(23), 2237–2245. <https://doi.org/10.1056/NEJMra1706158>
- Fox, M. D., Snyder, A. Z., Vincent, J. L., Corbetta, M., Van Essen, D. C., & Raichle, M. E. (2005). The human brain is intrinsically organized into dynamic, anticorrelated functional networks. *Proceedings of the National Academy of Sciences*, 102(27), 9673–9678. <https://doi.org/10.1073/pnas.0504136102>
- Friedman, L., & Komogortsev, O. V. (2019). Assessment of the effectiveness of seven biometric feature normalization techniques. *IEEE Transactions on Information Forensics and Security*, 14(10), 2528–2536. <https://doi.org/10.1109/TIFS.2019.2904844>
- Friston, K. J., Litvak, V., Oswal, A., Razi, A., Stephan, K. E., Van Wijk, B. C. M., ... Zeidman, P. (2016). Bayesian model reduction and empirical Bayes for group (DCM) studies. *NeuroImage*, 128, 413–431. <https://doi.org/10.1016/j.neuroimage.2015.11.015>
- Gogtay, N., Odonez, A., Herman, D. H., Hayashi, K. M., Greenstein, D., Vaituzis, C., ... Rapoport, J. L. (2007). Dynamic mapping of cortical development before and after the onset of pediatric bipolar illness. *Journal of Child Psychology and Psychiatry*, 48(9), 852–862. <https://doi.org/10.1111/j.1469-7610.2007.01747.x>
- Goulden, N., Khusnulina, A., Davis, N. J., Bracewell, R. M., Bokde, A. L., McNulty, J. P., & Mullins, P. G. (2014). The salience network is responsible for switching between the default mode network and the central executive network: Replication from DCM. *NeuroImage*, 99, 180–190. <https://doi.org/10.1016/j.neuroimage.2014.05.052>
- Greicius, M. D., Krasnow, B., Reiss, A. L., & Menon, V. (2003). Functional connectivity in the resting brain: A network analysis of the default mode hypothesis. *Proceedings of the National Academy of Sciences*, 100(1), 253–258. <https://doi.org/10.1073/pnas.0135058100>
- Gusnard, D. A., Akbudak, E., Shulman, G. L., & Raichle, M. E. (2001). Medial prefrontal cortex and self-referential mental activity: Relation to a default mode of brain function. *Proceedings of the National Academy of Sciences*, 98(7), 4259–4264. <https://doi.org/10.1073/pnas.071043098>
- Han, S., Zheng, R., Li, S., Liu, L., Wang, C., Jiang, Y., ... Cheng, J. (2023). Progressive brain structural abnormality in depression assessed with MR imaging by using causal network analysis. *Psychological Medicine*, 53(5), 2146–2155. <https://doi.org/10.1017/S0033291721003986>
- Harrison, P. J., Geddes, J. R., & Tunbridge, E. M. (2018). The emerging neurobiology of bipolar disorder. *Trends in Neurosciences*, 41(1), 18–30. <https://doi.org/10.1016/j.tins.2017.10.006>
- Hogeveen, J., Krug, M. K., Elliott, M. V., & Solomon, M. (2018). Insula-retrosplenial cortex overconnectivity increases internalizing via reduced insight in autism. *Biological Psychiatry*, 84(4), 287–294. <https://doi.org/10.1016/j.biopsych.2018.01.015>
- Jafri, M. J., Pearlson, G. D., Stevens, M., & Calhoun, V. D. (2008). A method for functional network connectivity among spatially independent resting-state components in schizophrenia. *NeuroImage*, 39(4), 1666–1681. <https://doi.org/10.1016/j.neuroimage.2007.11.001>
- Jain, A., Nandakumar, K., & Ross, A. (2005). Score normalization in multimodal biometric systems. *Pattern Recognition*, 38(12), 2270–2285. <https://doi.org/10.1016/j.patcog.2005.01.012>
- Johnson, W. E., Li, C., & Rabinovic, A. (2007). Adjusting batch effects in microarray expression data using empirical Bayes methods. *Biostatistics (Oxford, England)*, 8(1), 118–127. <https://doi.org/10.1093/biostatistics/kxj037>
- Kucyi, A., & Davis, K. D. (2014). Dynamic functional connectivity of the default mode network tracks daydreaming. *NeuroImage*, 100, 471–480. <https://doi.org/10.1016/j.neuroimage.2014.06.044>
- Lei, D., Li, W., Qin, K., Ai, Y., Tallman, M. J., Patino, L. R., ... DelBello, M. P. (2023). Effects of short-term quetiapine and lithium therapy for acute

- manic or mixed episodes on the limbic system and emotion regulation circuitry in youth with bipolar disorder. *Neuropsychopharmacology*, 48(4), 615–622. <https://doi.org/10.1038/s41386-022-01463-6>
- Li, Y., Wang, C., Teng, C., Jiao, K., Song, X., Tan, Y., ... Zhong, Y. (2019). Hippocampus-driving progressive structural alterations in medication-naïve major depressive disorder. *Journal of Affective Disorders*, 256, 148–155. <https://doi.org/10.1016/j.jad.2019.05.053>
- Lim, C. S., Baldessarini, R. J., Vieta, E., Yucel, M., Bora, E., & Sim, K. (2013). Longitudinal neuroimaging and neuropsychological changes in bipolar disorder patients: Review of the evidence. *Neuroscience & Biobehavioral Reviews*, 37(3), 418–435. <https://doi.org/10.1016/j.neubiorev.2013.01.003>
- Liu, C.-H., Ma, X., Wu, X., Zhang, Y., Zhou, F.-C., Li, F., ... Wang, C.-Y. (2013). Regional homogeneity of resting-state brain abnormalities in bipolar and unipolar depression. *Progress in Neuro-Psychopharmacology and Biological Psychiatry*, 41, 52–59. <https://doi.org/10.1016/j.pnpbp.2012.11.010>
- Liu, C., Pu, W., Wu, G., Zhao, J., & Xue, Z. (2019). Abnormal resting-state cerebral-limbic functional connectivity in bipolar depression and unipolar depression. *BMC Neuroscience*, 20(1), 30. <https://doi.org/10.1186/s12868-019-0508-6>
- Liu, G., Jiao, K., Zhong, Y., Hao, Z., Wang, C., Xu, H., ... Wang, C. (2021). The alteration of cognitive function networks in remitted patients with major depressive disorder: An independent component analysis. *Behavioural Brain Research*, 400, 113018. <https://doi.org/10.1016/j.bbr.2020.113018>
- Lopez-Larson, M. P., Shah, L. M., Weeks, H. R., King, J. B., Mallik, A. K., Yurgelun-Todd, D. A., & Anderson, J. S. (2017). Abnormal functional connectivity between default and salience networks in pediatric bipolar disorder. *Biological Psychiatry: Cognitive Neuroscience and Neuroimaging*, 2(1), 85–93. <https://doi.org/10.1016/j.bpsc.2016.10.001>
- Lu, Q.-Y., Towne, J. M., Lock, M., Jiang, C., Cheng, Z.-X., Habes, M., ... Zang, Y.-F. (2022). Toward coordinate-based cognition dictionaries: A BrainMap and neurosynth demo. *Neuroscience*, 493, 109–118. <https://doi.org/10.1016/j.neuroscience.2022.02.016>
- Luciano, M., Di Vincenzo, M., Mancuso, E., Marafioti, N., Di Cerbo, A., Giallonardo, V., ... Fiorillo, A. (2023). Does the brain matter? Cortical alterations in pediatric bipolar disorder: A critical review of structural and functional magnetic Resonance Studies. *Current Neuropsychopharmacology*, 21(6), 1302–1318. <https://doi.org/10.2174/1570159X20666220927114417>
- Lyoo, I. K., Sung, Y. H., Dager, S. R., Friedman, S. D., Lee, J., Kim, S. J., ... Renshaw, P. F. (2006). Regional cerebral cortical thinning in bipolar disorder. *Bipolar Disorders*, 8(1), 65–74. <https://doi.org/10.1111/j.1399-5618.2006.00284.x>
- Magioncalda, P., & Martino, M. (2022). A unified model of the pathophysiology of bipolar disorder. *Molecular Psychiatry*, 27(1), 202–211. <https://doi.org/10.1038/s41380-021-01091-4>
- Magioncalda, P., Martino, M., Conio, B., Escelsior, A., Piaggio, N., Presta, A., ... Amore, M. (2015). Functional connectivity and neuronal variability of resting state activity in bipolar disorder – reduction and decoupling in anterior cortical midline structures. *Human Brain Mapping*, 36(2), 666–682. <https://doi.org/10.1002/hbm.22655>
- Martino, M., & Magioncalda, P. (2022). Tracing the psychopathology of bipolar disorder to the functional architecture of intrinsic brain activity and its neurotransmitter modulation: A three-dimensional model. *Molecular Psychiatry*, 27(2), 793–802. <https://doi.org/10.1038/s41380-020-00982-2>
- McGrath, J. J., Al-Hamzawi, A., Alonso, J., Altwaijri, Y., Andrade, L. H., Bromet, E. J., ... Zaslavsky, A. M. (2023). Age of onset and cumulative risk of mental disorders: A cross-national analysis of population surveys from 29 countries. *The Lancet Psychiatry*, 10(9), 668–681. [https://doi.org/10.1016/S2215-0366\(23\)00193-1](https://doi.org/10.1016/S2215-0366(23)00193-1)
- McKenna, B. S., & Eyler, L. T. (2012). Overlapping prefrontal systems involved in cognitive and emotional processing in euthymic bipolar disorder and following sleep deprivation: A review of functional neuroimaging studies. *Clinical Psychology Review*, 32(7), 650–663. <https://doi.org/10.1016/j.cpr.2012.07.003>
- Menon, V. (2011). Large-scale brain networks and psychopathology: A unifying triple network model. *Trends in Cognitive Sciences*, 15(10), 483–506. <https://doi.org/10.1016/j.tics.2011.08.003>
- Menon, V. (2023). 20 years of the default mode network: A review and synthesis. *Neuron*, 111(16), 2469–2487. <https://doi.org/10.1016/j.neuron.2023.04.023>
- Mesbah, R., Koenders, M. A., Van Der Wee, N. J. A., Giltay, E. J., Van Hemert, A. M., & De Leeuw, M. (2023). Association between the fronto-limbic network and cognitive and emotional functioning in individuals with bipolar disorder: A systematic review and meta-analysis. *JAMA Psychiatry*, 80(5), 432. <https://doi.org/10.1001/jamapsychiatry.2023.0131>
- Mesulam, M. (1998). From sensation to cognition. *Brain*, 121(6), 1013–1052. <https://doi.org/10.1093/brain/121.6.1013>
- Mittner, M., Hawkins, G. E., Boekel, W., & Forstmann, B. U. (2016). A neural model of mind wandering. *Trends in Cognitive Sciences*, 20(8), 570–578. <https://doi.org/10.1016/j.tics.2016.06.004>
- Molnar-Szakacs, I., & Uddin, L. Q. (2022). Anterior insula as a gatekeeper of executive control. *Neuroscience & Biobehavioral Reviews*, 139, 104736. <https://doi.org/10.1016/j.neubiorev.2022.104736>
- Murray, E. A., Wise, S. P., & Graham, K. S. (2017). *The evolution of memory systems: Ancestors, anatomy, and adaptations: Vol. Chapter 1: The history of memory systems* (1st ed.). Oxford, UK: Oxford University Press.
- Najt, P., Nicoletti, M., Chen, H. H., Hatch, J. P., Caetano, S. C., Sassi, R. B., ... Soares, J. C. (2007). Anatomical measurements of the orbitofrontal cortex in child and adolescent patients with bipolar disorder. *Neuroscience Letters*, 413(3), 183–186. <https://doi.org/10.1016/j.neulet.2006.10.016>
- Nicenboim, B., Schad, D., & Vasishth, S. (2023). *An Introduction to Bayesian Data Analysis for Cognitive Science: Vol. 8.1.4*. <https://vasishth.github.io/bayescogsci/book/ch-contr.html#sec-cellMeans>
- Nierenberg, A. A., Agustini, B., Köhler-Forsberg, O., Cusin, C., Katz, D., Sylvia, L. G., ... Berk, M. (2023). Diagnosis and treatment of bipolar disorder: A review. *JAMA*, 330(14), 1370. <https://doi.org/10.1001/jama.2023.18588>
- Ong, D., Walterfang, M., Malhi, G. S., Styner, M., Velakoulis, D., & Pantelis, C. (2012). Size and shape of the caudate nucleus in individuals with bipolar affective disorder. *Australian & New Zealand Journal of Psychiatry*, 46(4), 340–351. <https://doi.org/10.1177/0004867412440191>
- Pavuluri, M. N., O'Connor, M. M., Harral, E., & Sweeney, J. A. (2007). Affective neural circuitry during facial emotion processing in pediatric bipolar disorder. *Biological Psychiatry*, 62(2), 158–167. <https://doi.org/10.1016/j.biopsych.2006.07.011>
- Perry, A., Roberts, G., Mitchell, P. B., & Breakspear, M. (2019). Connectomics of bipolar disorder: A critical review, and evidence for dynamic instabilities within interoceptive networks. *Molecular Psychiatry*, 24(9), 1296–1318. <https://doi.org/10.1038/s41380-018-0267-2>
- Philip, N. S., Barredo, J., Van 't Wout-Frank, M., Tyrka, A. R., Price, L. H., & Carpenter, L. L. (2018). Network mechanisms of clinical response to transcranial magnetic stimulation in posttraumatic stress disorder and major depressive disorder. *Biological Psychiatry*, 83(3), 263–272. <https://doi.org/10.1016/j.biopsych.2017.07.021>
- Phillips, M. L., Drevets, W. C., Rauch, S. L., & Lane, R. (2003). Neurobiology of emotion perception I: The neural basis of normal emotion perception. *Biological Psychiatry*, 54(5), 504–514. [https://doi.org/10.1016/S0006-3223\(03\)00168-9](https://doi.org/10.1016/S0006-3223(03)00168-9)
- Phillips, M. L., & Swartz, H. A. (2014). A critical appraisal of neuroimaging studies of bipolar disorder: Toward a new conceptualization of underlying neural circuitry and a road map for future research. *American Journal of Psychiatry*, 171(8), 829–843. <https://doi.org/10.1176/appi.ajp.2014.13081008>
- Power, J. D., Fair, D. A., Schlaggar, B. L., & Petersen, S. E. (2010). The development of human functional brain networks. *Neuron*, 67(5), 735–748. <https://doi.org/10.1016/j.neuron.2010.08.017>
- Rey, G., Piguet, C., Benders, A., Favre, S., Eickhoff, S., Aubry, J.-M., & Vuilleumier, P. (2016). Resting-state functional connectivity of emotion regulation networks in euthymic and non-euthymic bipolar disorder patients. *European Psychiatry*, 34, 56–63. <https://doi.org/10.1016/j.eurpsy.2015.12.005>
- Rocchi, G., Sterlini, B., Tardito, S., Inglese, M., Corradi, A., Filaci, G., ... Martino, M. (2020). Opioidergic system and functional architecture of intrinsic brain activity: Implications for psychiatric disorders. *The Neuroscientist*, 26(4), 343–358. <https://doi.org/10.1177/1073858420902360>
- Sabaroedin, K., Razi, A., Chopra, S., Tran, N., Pozaruk, A., Chen, Z., ... Fornito, A. (2023). Frontostriatal effective connectivity and dopaminergic function in the psychosis continuum. *Brain*, 146(1), 372–386. <https://doi.org/10.1093/brain/awac018>

- Sawyer, S. M., Azzopardi, P. S., Wickremarathne, D., & Patton, G. C. (2018). The age of adolescence. *The Lancet Child & Adolescent Health*, 2(3), 223–228. [https://doi.org/10.1016/S2352-4642\(18\)30022-1](https://doi.org/10.1016/S2352-4642(18)30022-1)
- Schaefer, A., Kong, R., Gordon, E. M., Laumann, T. O., Zuo, X.-N., Holmes, A. J., ... Yeo, B. T. T. (2018). Local-global parcellation of the human cerebral cortex from intrinsic functional connectivity MRI. *Cerebral Cortex*, 28(9), 3095–3114. <https://doi.org/10.1093/cercor/bhx179>
- Seeley, W. W., Menon, V., Schatzberg, A. F., Keller, J., Glover, G. H., Kenna, H., ... Greicius, M. D. (2007). Dissociable intrinsic connectivity networks for salience processing and executive control. *The Journal of Neuroscience*, 27(9), 2349–2356. <https://doi.org/10.1523/JNEUROSCI.5587-06.2007>
- Sha, Z., Wager, T. D., Mechelli, A., & He, Y. (2019). Common dysfunction of large-scale neurocognitive networks across psychiatric disorders. *Biological Psychiatry*, 85(5), 379–388. <https://doi.org/10.1016/j.biopsych.2018.11.011>
- Sharaev, M. G., Zavyalova, V. V., Ushakov, V. L., Kartashov, S. I., & Velichkovsky, B. M. (2016). Effective connectivity within the default mode network: Dynamic causal modeling of resting-state fMRI data. *Frontiers in Human Neuroscience*, 10, 14. <https://doi.org/10.3389/fnhum.2016.00014>
- Sridharan, D., Levitin, D. J., & Menon, V. (2008). A critical role for the right fronto-insular cortex in switching between central-executive and default-mode networks. *Proceedings of the National Academy of Sciences*, 105(34), 12569–12574. <https://doi.org/10.1073/pnas.0800005105>
- Starkstein, S. E., Fedoroff, P., Berthier, M. L., & Robinson, R. G. (1991). Manic-depressive and pure manic states after brain lesions. *Biological Psychiatry*, 29(2), 149–158. [https://doi.org/10.1016/0006-3223\(91\)90043-L](https://doi.org/10.1016/0006-3223(91)90043-L)
- Starkstein, S. E., Mayberg, H. S., Berthier, M. L., Fedoroff, P., Price, T. R., Dannals, R. F., ... Robinson, R. G. (1990). Mania after brain injury: Neuroradiological and metabolic findings. *Annals of Neurology*, 27(6), 652–659. <https://doi.org/10.1002/ana.410270612>
- Swann, A. C., Lijffijt, M., Lane, S. D., Steinberg, J. L., & Moeller, F. G. (2009). Increased trait-like impulsivity and course of illness in bipolar disorder. *Bipolar Disorders*, 11(3), 280–288. <https://doi.org/10.1111/j.1399-5618.2009.00678.x>
- Tost, H., Kolachana, B., Hakimi, S., Lemaitre, H., Verchinski, B. A., Mattay, V. S., ... Meyer-Lindenberg, A. (2010). A common allele in the oxytocin receptor gene (OXTR) impacts prosocial temperament and human hypothalamic-limbic structure and function. *Proceedings of the National Academy of Sciences*, 107(31), 13936–13941. <https://doi.org/10.1073/pnas.1003296107>
- Uddin, L. Q., Clare Kelly, A. M., Biswal, B. B., Xavier Castellanos, F., & Milham, M. P. (2009). Functional connectivity of default mode network components: Correlation, anticorrelation, and causality. *Human Brain Mapping*, 30(2), 625–637. <https://doi.org/10.1002/hbm.20531>
- Van Meter, A. R., Moreira, A. L. R., & Youngstrom, E. A. (2011). Meta-analysis of epidemiologic studies of pediatric bipolar disorder. *The Journal of Clinical Psychiatry*, 72(09), 1250–1256. <https://doi.org/10.4088/JCP.10m06290>
- Wade, B. S. C., Loureiro, J., Sahib, A., Kubicki, A., Joshi, S. H., Helleman, G., ... Narr, K. L. (2022). Anterior default mode network and posterior insular connectivity is predictive of depressive symptom reduction following serial ketamine infusion. *Psychological Medicine*, 52(12), 2376–2386. <https://doi.org/10.1017/S0033291722001313>
- Wessa, M., Perlino, C., & Brambilla, P. (2015). Neuropsychological underpinnings of the dynamics of bipolar disorder. *Epidemiology and Psychiatric Sciences*, 24(6), 479–483. <https://doi.org/10.1017/S2045796015000098>
- Whitfield-Gabrieli, S., & Ford, J. M. (2012). Default mode network activity and connectivity in psychopathology. *Annual Review of Clinical Psychology*, 8(1), 49–76. <https://doi.org/10.1146/annurev-clinpsy-032511-143049>
- Wilke, M., Kowatch, R. A., DelBello, M. P., Mills, N. P., & Holland, S. K. (2004). Voxel-based morphometry in adolescents with bipolar disorder: First results. *Psychiatry Research: Neuroimaging*, 131(1), 57–69. <https://doi.org/10.1016/j.pscychresns.2004.01.004>
- Wu, Y.-K., Su, Y.-A., Li, L., Zhu, L.-L., Li, K., Li, J.-T., ... Si, T.-M. (2023). Brain functional changes across mood states in bipolar disorder: From a large-scale network perspective. *Psychological Medicine*, 54(4), 763–774. <https://doi.org/10.1017/S0033291723002453>
- Yan, C.-G., Wang, X.-D., Zuo, X.-N., & Zang, Y.-F. (2016). DPABI: Data processing & analysis for (Resting-State) brain imaging. *Neuroinformatics*, 14(3), 339–351. <https://doi.org/10.1007/s12021-016-9299-4>
- Yokoyama, S., Okamoto, Y., Takagaki, K., Okada, G., Takamura, M., Mori, A., ... Yamawaki, S. (2018). Effects of behavioral activation on default mode network connectivity in subthreshold depression: A preliminary resting-state fMRI study. *Journal of Affective Disorders*, 227, 156–163. <https://doi.org/10.1016/j.jad.2017.10.021>
- Zarp Petersen, J., Varo, C., Skovsen, C. F., Ott, C. V., Kjaerstad, H. L., Vieta, E., ... Miskowiak, K. W. (2022). Neuronal underpinnings of cognitive impairment in bipolar disorder: A large data-driven functional magnetic resonance imaging study. *Bipolar Disorders*, 24(1), 69–81. <https://doi.org/10.1111/bdi.13100>
- Zeidman, P., Jafarian, A., Corbin, N., Seghier, M. L., Razi, A., Price, C. J., & Friston, K. J. (2019a). A guide to group effective connectivity analysis, part 1: First level analysis with DCM for fMRI. *NeuroImage*, 200, 174–190. <https://doi.org/10.1016/j.neuroimage.2019.06.031>
- Zeidman, P., Jafarian, A., Seghier, M. L., Litvak, V., Cagnan, H., Price, C. J., & Friston, K. J. (2019b). A guide to group effective connectivity analysis, part 2: Second level analysis with PEB. *NeuroImage*, 200, 12–25. <https://doi.org/10.1016/j.neuroimage.2019.06.032>
- Zhang, D., & Raichle, M. E. (2010). Disease and the brain's dark energy. *Nature Reviews Neurology*, 6(1), 15–28. <https://doi.org/10.1038/nrneurol.2009.198>
- Zhang, Z., Bo, Q., Li, F., Zhao, L., Wang, Y., Liu, R., ... Zhou, Y. (2022). Altered effective connectivity among core brain networks in patients with bipolar disorder. *Journal of Psychiatric Research*, 152, 296–304. <https://doi.org/10.1016/j.jpsychires.2022.06.031>
- Zhou, Y., Friston, K. J., Zeidman, P., Chen, J., Li, S., & Razi, A. (2018). The hierarchical organization of the default, dorsal attention and salience networks in adolescents and young adults. *Cerebral Cortex*, 28(2), 726–737. <https://doi.org/10.1093/cercor/bhx307>
- Zovetti, N., Rossetti, M. G., Perlino, C., Maggioni, E., Bontempi, P., Bellani, M., & Brambilla, P. (2020). Default mode network activity in bipolar disorder. *Epidemiology and Psychiatric Sciences*, 29, e166. <https://doi.org/10.1017/S2045796020000803>